Journal of Photochemistry and Photobiology, B: Biology, 5 (1990) 121 - 126

News and Views

Tumor Oxygen Tension During Photodynamic Therapy

B. J. TROMBERG, S. KIMEL, A. ORENSTEIN, S. J. BARKER, J. HYATT, J. S. NELSON, W. G. ROBERTS and M. W. BERNS

Beckman Laser Institute and Medical Clinic, University of California at Irvine, Irvine, CA 92715 (U.S.A.)

1. Introduction

The administration of a sufficient dose of radiation at the appropriate wavelength to photosensitizer-containing neoplasms is essential for photodynamic therapy (PDT). Accordingly, monitoring the effects of light delivery in tissue during PDT has great clinical significance.

In order to understand PDT on the molecular level, one or more "participants" (*e.g.* reaction products or intermediates) in the photodynamic reactions have to be measured. We will concentrate on the role of oxygen as a participant since PDT has been shown to depend critically, although in a rather complicated way, on the presence of oxygen [1].

Three consecutive processes can be distinguished. In the first phase, PDT involves the photogeneration of cytotoxic oxygen intermediates, primarily singlet molecular oxygen $^1O_2$, at the expense of ground state molecular oxygen O_2, which by photochemical processes cause damage to essential cellular components. In this "oxidative" phase, the presence of oxygen is crucial for the initiation of PDT. The photo-oxidation reactions cause a dynamic, reversible depletion of ambient oxygen which is proportional to the fluence rate.

In the second phase, oxygen-induced pathophysiological alterations lead to occlusion of blood vessels and hypoxia [2 - 4]. During this stage, measurements of oxygen reflect a depletion of tissue oxygen because of the decreased supply. For low light doses the "hypoxic" phase is reversible, since in the absence of light the blood flow is restored.

In the third phase of *in vivo* PDT, regional breakdown of oxygen and nutrient delivery occurs due to vascular collapse which causes tumor necrosis [4]. In this "ischemic" stage the depletion of oxygen levels is, of course, irreversible. Even if the exact role of oxygen in each phase is still being debated, it is clear that the progress of PDT can be followed by monitoring tissue oxygen depletion.

Most *in vivo* studies have dealt in a descriptive fashion with photodynamic reactions in the third phase. These efforts have used histological techniques [5 - 7]. observation chambers [4] or blood flow measurements

1011-1344/90/$3.50

[8, 9] to assess the influence of PDT on tumor microvasculature. They thus provide information, indirectly, about the mechanism(s) of PDT.

Direct measurements of oxygen during the early phases of PDT have been carried out by monitoring the *in vivo* depletion of oxygen with an oxygen electrode implanted in the tumor or tissue [10] or by following pharmacological changes in a chemical marker for oxygen [11]. Drawbacks to these techniques include (i) the possibility that electrode-induced bleeding, edema and vasoconstriction may distort tissue oxygen levels and (ii) the lack of rapid, "real time" information from the chemical indicator.

In an effort to understand more clearly the primary events which lead to tumor destruction, we have employed transcutaneous oxygen sensors [12] for non-invasive monitoring of transcutaneous oxygen tension ($PtcO_2$) at the site of the tumor during PDT. The progress of PDT can be followed in real time, thus permitting a fast, semi-quantitative evaluation of the efficiency of PDT as a function of energy dose.

2. *Experimental procedure*

Male New Zealand white rabbits were selected because they possess large, thin, well-vascularized ears in which subcutaneous tumors can be implanted and sufficient vascularization is available to support tumor growth. VX-2 skin carcinoma tumor cells were introduced intradermally into the dorsal medial portion of the ear. A total of 11 animals had tumor implants in their right ears. Within 2 days of implantation, newly formed blood vessels penetrated the tumor centripetally from the adjacent, normal vasculature. Once vascularized, the tumor grew rapidly to a size of 7 - 10 mm by day 5 at which time the experiment was started. Intravenous injections of Photofrin II (PII, 10 mg kg^{-1} body weight) were administered 24 h prior to irradiation. Seven animals received intravenous PII injections via marginal ear veins, while four controls did not receive PII.

After administration of anesthesia, three transcutaneous, Clark-type oxygen electrodes (Novametrix model 807), each 1.5 cm^2 in area, were applied to the dorsal side of the ears. On the right (tumor) ear, two electrodes were attached, one on top of the tumor and the second adjacent to the tumor. On the left ear, a single electrode was placed adjacent to the medial artery. The electrodes were affixed to the skin with double-sided tape. The electrode contains a heating unit which heats the skin surface to 44 °C, thus effectively "melting" the stratum–corneum-layer barrier to diffusion of oxygen [12]. An oxygen mask was positioned over the animal's face and flow was adjusted until a stable $PtcO_2$ baseline in the 100 Torr region was established (this typically required 15 - 30 min).

Irradiations were performed using an argon-pumped dye laser tuned to 630 nm. The dye laser output was focused onto a quartz optical fiber (diameter, 400 μm) and the fiber tip distance from the target tissue was adjusted so that a spot 1.5 cm in diameter was irradiated perpendicular to the surface.

The radiation was incident on the ventral side and penetrated through the ear to the tumor (on the dorsal side). The incident power density at the target tissue was 500 W m^{-2}. During phototherapy 200 kJ m^{-2} was delivered to the tissue.

Laser light was directed to the tumor (right ear) and the response of all three electrodes was recorded simultaneously. This was followed by irradiation at the (non-tumor) electrode site on the left ear. The response of the left-ear electrode was recorded simultaneously with that of the control electrode on the right ear. The response of all electrodes was registered with strip chart recorders during irradiation and for an additional 10 min after irradiation.

3. Results and discussion

Typical results for a fluence of 200 kJ m^{-2} during a single 400 s period are presented in Fig. 1. In order to obtain the relative oxygen pressure values (%), the measured $PtcO_2$ values were divided by the average starting level (baseline) $PtcO_2$ measurement. The data demonstrate that irradiation of both the tumor (Fig. 1(a)) and non-tumor (Fig. 1(b)) ears rapidly elicits drastic reductions in $PtcO_2$ values at the irradiation site. In the case of non-tumor irradiations, the electrode response is generally slower and less severe: $PtcO_2$ levels do not reach zero and post-irradiation values generally return to baseline. Presumably, these results can be attributed to differences in vasculature and PII concentration between tumor and non-tumor sites. The control electrodes display constant $PtcO_2$ levels, thus underscoring the site specificity of tissue oxygen variations. Irradiation of drug-free control animals results in stable (baseline) $PtcO_2$ readings (not shown).

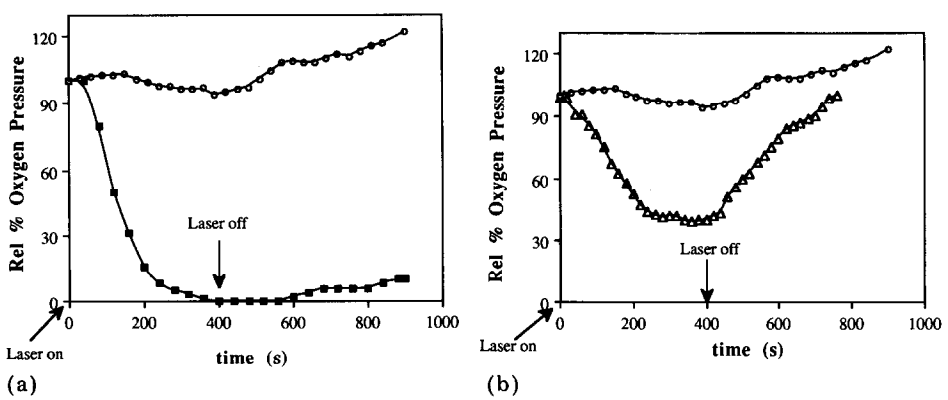

Fig. 1. Electrode response for experimental rabbit: (a) irradiation of tumor (right) ear; (b) irradiation of non-tumor (left) ear. Electrode locations: ■, tumor electrode, right ear; ○, electrode adjacent to tumor, right ear; △, electrode on non-tumor (left) ear.

Dynamic effects which contribute to changes in $PtcO_2$ are illustrated in Fig. 2. These factors were investigated by subjecting rabbits to short-term irradiations (100 s, 50 kJ m^{-2} fluence), interspersed with 200 s "laser-off" segments. Total fluence was at least 250 kJ m^{-2}. The results show that the $PtcO_2$ fall-off is coincident with irradiation. In the first few dark periods, $PtcO_2$ values tend to return to pre-irradiation levels, indicating "oxidative phase" processes. However, as the cumulative radiation dose increases, tumor $PtcO_2$ values approach zero (Fig. 2(a)) after 1200 - 1300 s (elapsed time). This corresponds to a cumulative fluence of 250 kJ m^{-2}, suggesting permanent collapse of microvasculature ("ischemic phase"). In contrast, delivery of equivalent radiation doses to the non-tumor ear results in temporary oxygen depletion due to "oxidative" and "hypoxic" processes followed by partial replenishment of oxygen during dark periods (Fig. 2(b)). This is consistent with the observed overall differences in PDT response between tumor and non-tumor ears.

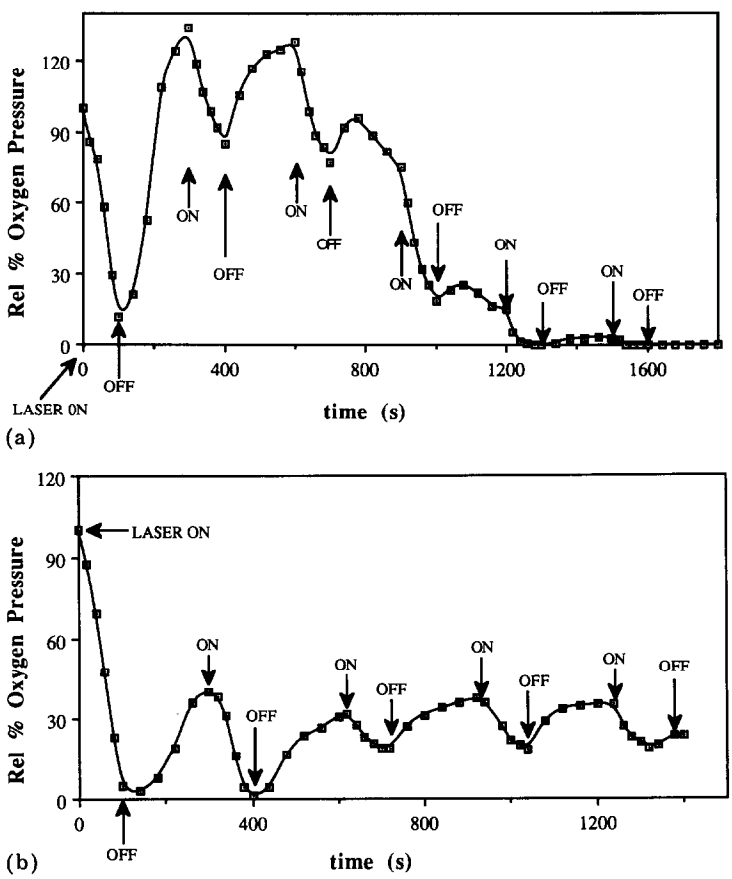

Fig. 2. Time-dependent electrode response at irradiation site for experimental animals: (a) tumor (right) ear; (b) non-tumor (left) ear. Irradiation conditions: laser on for 100 s (50 kJ m^{-2}, 630 nm) followed by laser off for 200 s.

The most probable explanations for our observations include photodynamic oxygen consumptive processes and rapid, reversible occlusive events, *e.g.* hemodynamic disturbances. Since $PtcO_2$ reflects oxygen delivery to tissue [13], *in vivo* $PtcO_2$ should be considered as a gauge which, continuously and non-invasively, measures two factors; these are photochemistry and blood flow; the combined impact of which is indicative of PDT efficiency.

During the first 100 - 200 s of irradiation (50 - 100 kJ m^{-2}), $PtcO_2$ measurements (Fig. 1) clearly demonstrate rapid tissue oxygen depletion. It has been reported that for these low light doses there may be small changes in blood flow [9]. In spite of this, the relatively minor effects on vasculature and thus on blood flow (within the first few seconds of irradiation) have a negligible influence on $PtcO_2$ levels. Thus the rate of oxygen consumed by the tissue due to photodynamics can be determined.

In contrast with low light dose conditions, where there are only minor blood flow changes, larger cumulative radiation doses lead to considerable reductions in blood velocity [8, 9]. From a practical standpoint, this makes it difficult to estimate the amount of oxygen consumed by the tissue. In this case, $PtcO_2$ measurements effectively monitor the state of circulation, rather than the absolute oxygen tension, and reveal the extent to which regional breakdowns in oxygen delivery occur. For example, reductions in $PtcO_2$ could be indicative of tumor hypoxia induced by microvascular changes.

The cyclic nature of $PtcO_2$ reduction as a function of time for recurrent irradiation (Fig. 2) may provide a clue to the dynamics of PDT. These results suggest sludging and aggregation of erythrocytes in the "on-time", followed by restored erythrocyte flow during the dark periods. Moreover, the $PtcO_2$ "overshoot" during "laser-off" intervals may be due to vasodilation which can occur as a compensatory response of the organism to a sudden reduction of oxygen in the measured region. When relatively small doses of light are absorbed, local flow changes may be sufficiently minor so that the difference between maximum and minimum $PtcO_2$ values during the course of irradiation could reflect the amount of oxygen utilized by the tissue.

Clearly, large light fluences (200 kJ m^{-2}) significantly influence blood flow during PDT. Sustained irradiation of PII-containing tissues results in structural alteration of the vasculature, blood flow reduction, tumor hypoxia and, ultimately, necrosis. These effects are illustrated by the overall downward trend of $PtcO_2$ in Fig. 2. With each energy dose, there is additional destruction and, eventually, $PtcO_2$ levels reflect the flow status of the vessels. Therefore the exact amount of oxygen consumed by the irradiated tissue is difficult to determine for large, structure-altering energy doses.

In conclusion, we have, for the first time, followed the progress of PDT *in vivo* by non-invasive monitoring for oxygen depletion. Although an exact relationship between tissue oxygen consumption and $PtcO_2$ is difficult to determine, it is possible to estimate PDT-induced oxygen consumption. Even though the exact nature of $PtcO_2$ fluctuations is still not completely understood, it is a valuable measure of the clinical effectiveness of PDT, since it is

indicative of changes in oxygen delivery at the irradiated site. In this manner it may be possible to utilize $PtcO_2$ measurements as a general *in situ* predictor of the radiant energy required to elicit irreversible tumor damage.

1 B. W. Henderson and V. H. Fingar, Relationship of tumor hypoxia and response to photodynamic treatment in an experimental mouse tumor, *Cancer Res.*, *47* (1987) 3110 - 3114.

2 J. P. Thomas, R. D. Hall and A. W. Girotti, Singlet oxygen intermediacy in the photodynamic action of membrane-bound hematoporphyrin derivative, *Cancer Lett.*, *35* (1987) 295 - 302.

3 J. S. Nelson, L.-H. Liaw and M. W. Berns, Tumor destruction in photodynamic therapy, *Photochem. Photobiol.*, *46* (1987) 829 - 835.

4 W. M. Star, H. P. A. Marijnissen, A. E. van der Berg-Block, J. A. C. Versteeg, K. A. P. Franken and H. S. Reinhold, Destruction of rat mammary tumor and normal tissue microcirculation by hematoporphyrin derivative photoradiation observed *in vivo* in sandwich observation chambers, *Cancer Res.*, *46* (1986) 2532 - 2540.

5 K. Chaudhuri, R. W. Keck and S. H. Selman, Morphological changes of tumor microvasculature following hematoporphyrin derivative sensitized photodynamic therapy, *Photochem. Photobiol.*, *46* (1987) 823 - 827.

6 C.-W. Lin, T. Amano, A. R. Rutledge, J. R. Shulok and G. R. Prout, Photodynamic effect in an experimental bladder tumor treated with intratumor injection of hematoporphyrin derivative, *Cancer Res.*, *48* (1988) 6115 - 6120.

7 J. S. Nelson, L.-H. Liaw, A. Orenstein, W. G. Roberts and M. W. Berns, Mechanism of tumor destruction following photodynamic therapy with hematoporphyrin derivative, chlorin and phthalocyanine, *J. Natl. Cancer Inst.*, *80* (1988) 1599 - 1605.

8 S. H. Selman, M. Kreimer-Birnbaum, J. E. Klaunig, P. J. Goldblatt, R. W. Keck and S. L. Britton, Blood flow in transplantable bladder tumors treated with hematoporphyrin derivative and light, *Cancer Res.*, *44* (1984) 1924 - 1927.

9 T. J. Wieman, T. S. Mang, V. H. Fingar, T. G. Hill, M. W. R. Reed, R. S. Corey, V. Q. Nguyen and E. R. Render, Effect of photodynamic therapy on blood flow in normal and tumor vessels, *Surgery*, *104* (1988) 512 - 517.

10 F. W. Hetzel and H. Farmer, Dose effect relationships in a mouse mammary tumor, in D. R. Doiron and C. J. Gomer (eds.), *Porphyrin Localization and Treatment of Tumors*, Alan R. Liss, New York, 1984, pp. 583 - 590.

11 B. D. Hirsch, N. C. Walz, B. E. Meeker, M. R. Arnfield, J. Tulip, M. S. McPhee and J. D. Chapman, Photodynamic therapy-induced hypoxia in rat tumors and normal tissues, *Photochem. Photobiol.*, *46* (1987) 847 - 852.

12 S. J. Barker and K. K. Tremper, Intra-arterial oxygen tension monitoring, *Int. Anesthesiol. Clin., Adv. Oxygen Monitoring*, *25* (1987) 199 - 208.

13 D. W. Lubbers, Theoretical basis of the transcutaneous blood gas measurements, *Crit. Care Med.*, *9* (1981) 721 - 733.